Aggregation of double-tail sulfonate surfactants probed by sodium-23 NMR

ARTICLE *in* THE JOURNAL OF PHYSICAL CHEMISTRY · APRIL 1984

Impact Factor: 2.78 · DOI: 10.1021/j150652a042

Reprinted from The Journal of Physical Chemistry, 1984, 88, 1649.

Aggregation of Double-Tail Sulfonate Surfactants Probed by ^{23}Na NMR

Peter K. Kilpatrick and Wilmer G. Miller*

Departments of Chemical Engineering and Materials Science and of Chemistry, University of Minnesota, Minneapolis, Minnesota 55455 *(Received: May 25, 1983; In Final Form: September 15, 1983)*

Analysis of sodium-23 NMR chemical shift and line-width data on sodium 4-(1-heptylnonyl)benzenesulfonate (SHBS) in water at 47 °C indicates the surfactant continuously aggregates in an anti- or weakly cooperative manner up to the surfactant solubility limit, a point beyond which a hydrated lamellar phase is in equilibrium with the surfactant-saturated isotropic solution. By contrast, sodium bis(2-ethylhexyl) sulfosuccinate (Aerosol OT) shows little if any aggregation up to the point of a highly cooperative micellization. Both chemical shift and line-width data indicate the presence of an isotropic solution–liquid crystal phase boundary; the line shape of a biphasic mixture of isotropic solution and lamellar liquid crystal is not motionally averaged, in contrast to a micellar solution, and thus differentiation between micelle formation and a solubility boundary is possible. A multiple equilibrium treatment of stepwise amphiphile aggregate formation is used to model both highly cooperative surfactant association, i.e. micellization, and anti- or noncooperative association. We model sodium counterion binding to surfactant aggregates by assuming the oligomers are spherical and have a constant surface charge density with all anionic head groups residing at the surface of the sphere. We then assume that the sodium ion exists in one of two environments: free or bound, each having a characteristic chemical shift and transverse relaxation rate. On the basis of a comparison of the model with experimental data, we conclude that SHBS aggregate concentration decreases with increasing aggregate size; i.e., the aggregation is non- or weakly anticooperative, while Aerosol OT associates very cooperatively, the large degree of cooperativity being an indication of micelle formation.

Introduction

At low concentrations in water, surfactants are molecularly dispersed like other solutes. As concentration increases, the surfactant may organize into micelles or it may separate as an ordered phase, either crystalline or liquid crystalline. The behavior observed depends on a variety of structural properties and thermodynamic variables, most important of which are the number, length, and branching of the hydrophobic surfactant moieties and the temperature.

There is convincing evidence from both surface tension[1,2] and conductance data[3] that sodium bis(2-ethylhexyl) sulfosuccinate (Aerosol OT) forms micelles at surfactant concentrations greater than 2.5×10^{-3} M in water at 20 °C. At still higher concentrations liquid-crystalline phases appear.[3,4] Many other double-tail sulfosuccinates also micellize.[1,2] The behavior of another homologous series, the dialkanoyl phosphatidylcholines, depends on the lipophilic group chain length. Short-chain homologues micellize, while in higher homologues a lamellar phase boundary is reached before micellization occurs.[5-8]

Previous studies[9] of sodium 4-(1-heptylnonyl)benzenesulfonate, SHBS, found a solubility limit at 25 °C of ca. 0.06 wt %, which increases to only 0.5 wt % at 90 °C. Such a low and temperature-insensitive solubility limit indicates that SHBS is below its Krafft boundary at 90 °C; consequently, micelles may be absent. Conductance data support this conclusion.[10,11] Recently, Magid and co-workers[12,13] have suggested that SHBS forms micelles with an apparent spherical radius of 23 Å (17-Å Guinier radius) in water at 45 °C, above a critical micelle concentration of 6.7×10^{-4} M (ca. 0.027 wt %). Their evidence for a cmc is drawn from conductance data.[12] The aggregate size is determined from small-angle neutron scattering.[13]

In this paper we investigate the state of aggregation of the double-tail surfactants SHBS and Aerosol OT, as well as sodium dodecyl sulfate (SDS) as a point of reference, by ^{23}Na NMR spectroscopy. Gustavsson and Lindman showed that the sodium counterions of anionic single-tail surfactants undergo a change in both transverse relaxation time and chemical shift upon micelle formation.[14-16] Up to the cmc the chemical shift (or relaxation rate) is nearly that of dilute sodium ions in water and differs from the corresponding value of micelle-bound counterions. Above the cmc (c_{cmc}) the chemical shift was approximated in their work by a two-state phase-separation model, characterized at total surfactant concentration c_t by a chemical shift (or line width) of micelle-bound sodium ions (δ_b), one for free ions (δ_f), and rapid exchange between the two populations:

$$\delta = \delta_f + \beta(\delta_b - \delta_f) - \frac{\beta c_{cmc}}{c_t}(\delta_b - \delta_f) \qquad (1)$$

where β, the fractional degree of counterion binding to the micelle, is assumed to be independent of concentration. This model assumes only two states of surfactant exist: unassociated surfactant monomer with free counterion and micellar aggregate of infinite size with bound counterions and fixed fractional charge. Moreover, the chemical shifts corresponding to these two states are assumed to be independent of concentration. The assumption of concentration independence of β and treatment of micelle formation as a phase separation are reasonable to the extent that the experimental counterion chemical shift and relaxation data are concentration independent up to a cmc and then break with a discontinuity in slope and become linear in inverse concentration. Of course, this is never strictly true.

(1) E. F. Williams, N. T. Woodberry, and J. K. Dixon, *J. Colloid Sci.*, **12**, 452 (1957).
(2) S. V. Rudenko, K. O. Averbakh, O. K. Smirmov, and S. M. Levi, *Colloid J. USSR (Engl. Transl.)* **30**, 312 (1968).
(3) K. Fontell, *J. Colloid Interface Sci.*, **44**, 318 (1973).
(4) J. Rogers and P. A. Winsor, *J. Colloid Interface Sci.*, **30**, 247 (1969).
(5) R. J. M. Tausk, J. Karmiggelt, C. Oudshoorn, and J. Th. G. Overbeek, *Biophys. Chem.*, **1**, 175 (1974).
(6) R. J. M. Tausk, J. VanEsch, J. Karmiggelt, C. Voordouw, and J. Th. G. Overbeek, *Biophys. Chem.*, **1**, 184 (1974).
(7) C. Tanford, "The Hydrophobic Effect", Wiley-Interscience, New York, 1978.
(8) S. Mabrey and J. M. Sturtevant, *Proc. Natl. Acad. Sci. U.S.A.*, **73**, 3862 (1976).
(9) E. I. Franses, H. T. Davis, W. G. Miller, and L. E. Scriven in "Chemistry of Oil Recovery", R. T. Johansen and R. L. Berg, Eds., American Chemical Society, Washington, DC, 1979, ACS Symp. Ser. No. 91, p 35.
(10) J. E. Puig, Ph.D. Thesis, University of Minnesota, 1982.
(11) J. E. Puig, H. T. Davis, L. E. Scriven, and W. G. Miller in "Interfacial Phenomena in Enhanced Oil Recovery", D. Wasan and A. Payatakes, Eds., American Institute of Chemical Engineers, New York, 1982, AIChE Symp. Ser. S-212, p 1.
(12) L. J. Magid, R. J. Shaver, E. Gulari, B. Bedwell, and S. Alkhafaji, *Prepr. Div. Pet. Chem., Am. Chem. Soc.*, **26**, 93 (1981).
(13) L. J. Magid, R. Triolo, J. S. Johnson, Jr., and W. C. Koehler, *J. Phys. Chem.*, **86**, 164 (1982).
(14) H. Gustavsson and B. Lindman, *J. Chem. Commun.*, 93 (1973).
(15) H. Gustavsson and B. Lindman, *J. Am. Chem. Soc.*, **97**, 3923 (1975).
(16) H. Gustavsson and B. Lindman, *J. Am. Chem. Soc.*, **100**, 4647 (1978).

0022-3654/84/2088-1649$01.50/0

A more realistic model of aggregation must admit dynamic equilibrium among aggregates of all sizes. Furthermore, the fractional degree of counterion binding, β, must vary with aggregate size, particularly among small aggregates. Amphiphile aggregate formation is modeled with stepwise addition reactions, treating two distinct cases: anti- or weakly cooperative association for all aggregate sizes and strongly cooperative association for a narrow domain of aggregate sizes, i.e. micellization. Counterion binding to surfactant aggregates is modeled by assuming the oligomers are spherical and have a constant surface charge density with all anionic head groups residing on the surface of the sphere. To test the sensitivity of chemical shifts and transverse relaxation rates on this constant surface charge density assumption, we also consider a step function change in β as aggregate size increases.

The ^{23}Na chemical shift and relaxation rate in a lamellar liquid-crystalline phase are also different from those in a molecular or micellar solution.[17] Although chemical exchange of counterions between the lamellar and isotropic phases is on the order of or slower than the time scale of the NMR experiment (ca. 0.01 or 0.1 s), superposition of the individual line shapes upon phase separation leads to a change in chemical shift (or line width). With biphasic systems in which a lamellar phase coexists with an isotropic phase over a large range in surfactant concentration, the observed chemical shift or relaxation rate as concentration increases must ultimately approach that of the bulk lamellar phase. This assumes that the morphology of the lamellar phase in a biphasic dispersion does not affect its chemical shift. With systems in which a two-phase region exists over a small range in concentration followed by a sizeable single lamellar phase of varying composition such as in Aerosol OT, one might anticipate that the ^{23}Na chemical shift continues to change as composition within the bulk lamellar phase is varied.

Both ^{23}Na chemical shifts and line half-widths (or transverse relaxation rates) change upon aggregation and also upon separation of a lamellar liquid-crystalline phase. The type of aggregation can be determined through a combination of line-width, line-shape, and chemical shift data in the case of the two double-tail surfactants, SHBS and Aerosol OT. We extend Lindman, Danielsson, and Gustavsson's model of chemical shift and relaxation rate changes[14-16,18] upon micelle formation and consider other less cooperative types of surfactant aggregation by using a mass action model of amphiphile association. Our model accounts for all sizes of aggregates that are in dynamic equilibrium and directly implements strong, weak, or anticooperativity of association in the prediction of these spectroscopic properties.

Experimental Section

Aerosol OT was obtained from Fluka AG, Buchs SG, Switzerland, in purum grade (>98%) and was used without further purification. SDS was obtained from BDH Chemicals in "specially pure" form and was used as received. SHBS was from the University of Texas, Austin, and purified according to the procedure described by Franses et al.[9] The NaCl was Fisher Scientific certified ACS grade and was dried at 110 °C immediately before use. The water was doubly distilled and then drawn through a four-stage Millipore cartridge system until its specific conductivity was less than 5×10^{-7} S/cm.

^{23}Na NMR spectra were taken on a Varian XL-100 spectrometer operating in the FT mode at 26.47 MHz. Chemical shifts were measured relative to an external reference solution of sodium tetraphenylboron in CD_3CN, which was inserted coaxially. With most samples the experimental uncertainty in chemical shifts was about ±0.01 ppm. The uncertainty was contributed to by temperature-dependent chemical shifts, spectral resolution, and reference peak resolution. With liquid-crystalline samples at higher surfactant concentrations, the change of magnetic susceptibility with concentration produces an additional chemical shift uncertainty. This uncertainty is negligible at low concentrations ($<10^{-2}$ M) at which most measurements were made. A 2000-Hz spectral window with 4096 data points and an acquisition time of 1.0 s was used for most samples. The number of transients which gave adequate peak resolution varied from about 2000 for the most concentrated samples to 100 000 or more for the most dilute samples. Transverse relaxation rates were determined from the full width at half-height ($\Delta\nu_{1/2}$) of the absorption mode spectrum taken directly from the spectrum and corrected for sensitivity enhancement. The uncertainty in $\Delta\nu_{1/2}$ was estimated at ±1 Hz for most samples, although the contribution to transverse relaxation rates from magnetic field inhomogeneity did vary from sample to sample. This was checked periodically by running a dilute NaCl solution whose line half-width is known accurately. With some samples, chemical shifts were accurately determined while line widths were not, due to variations in field homogeneity. Similarly, with some samples, line widths were accurately determined while chemical shifts were not, due to uncertainties in reference peak resolution. With Aerosol OT and SHBS, the temperature was maintained at 47 ± 1 °C by rapidly blowing thermostated nitrogen around the sample probe. Aqueous solutions of SDS were run at 25 ± 1 °C.

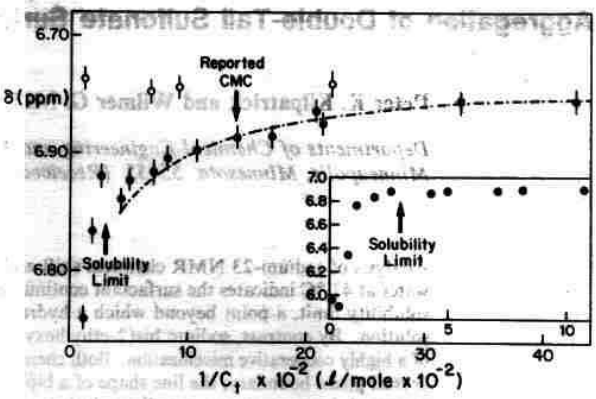

Figure 1. Concentration dependence of ^{23}Na chemical shift in SHBS–H_2O (●) and in NaCl–H_2O (○) at 47 °C. The solubility limit, determined by turbidity at 47 °C, and the reported[12,13] cmc at 45 °C are indicated. The dashed line was calculated from eq 4–6 by using $K(n) = 5 \times 10^4 \exp(-1 \times 10^{-5}(n-2)^2)$ or $K(n) = 3 \times 10^4 \exp(-3 \times 10^{-4}(n-25)^2)$.

Experimental Results

The ^{23}Na NMR chemical shift of SHBS in water at 47 °C as a function of inverse surfactant concentration is shown in Figure 1, where the chemical shift is reported as the position of maximum signal intensity. Also shown are the estimated solubility limit of SHBS at 47 °C as determined from visible turbidity, the chemical shift of dilute NaCl solutions at 47 °C, and the quoted cmc of Magid et al.[12] at 45 °C. A noteworthy feature of the chemical shift data is an abrupt change in slope near the estimated solubility limit of $1/c_t = 300$ L/mol ($c_t = 3.3 \times 10^{-3}$ M). Below the solubility limit, the chemical shift changes monotonically and smoothly, asymptotically approaching the value of dilute electrolyte at sufficiently low concentrations. This indicates a smooth and continuous change in the average environment of the sodium counterions, a situation consistent with aggregation of the surfactant in a non- or anticooperative fashion. By cooperative, we mean that the aggregate inventory exhibits a peak with increasing aggregate size. This picture of association agrees with Magid et al.'s conductance data[12] and data from our own laboratory,[10,11] which show a continuous variation of equivalent conductivity greater than that predicted by Onsager limiting law behavior, but which show no sharp break with increasing concentration which could be interpreted as evidence of micelle formation.

In addition to the chemical shift data, an isotropic–lamellar liquid-crystal phase boundary is indicated by the change in spectral line width and shape. At concentrations below the solubility limit, as indicated by visible turbidity, the ^{23}Na NMR line shapes are

(17) P. K. Kilpatrick et al. in "Microemulsions", I. D. Robb, Ed., Plenum Press, 1982, p 144.
(18) B. Lindman and I. Danielsson, *J. Colloid Interface Sci.*, **39**, 349 (1972).

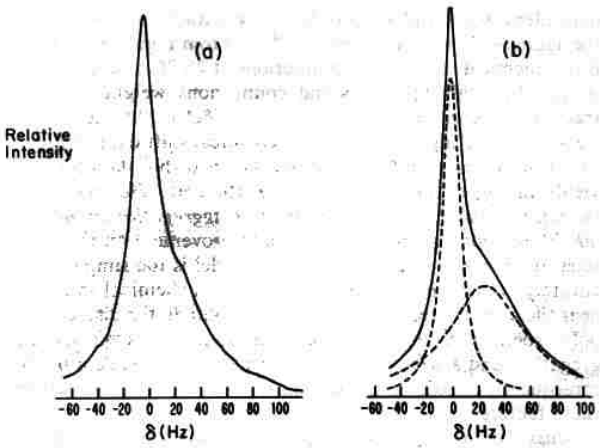

Figure 2. (a) The ^{23}Na spectrum of 0.355 wt % SHBS in water at 47 °C. The sample was noticeably turbid. (b) Superposition of two Lorentzian line shapes, saturated isotropic SHBS solution of $\Delta\nu$ = 16 Hz centered at 0 Hz and lamellar phase of $\Delta\nu_{1/2}$ = 70 Hz centered at 25.9 Hz, using a surfactant inventory of 40% in isotropic phase and 60% in lamellar phase.

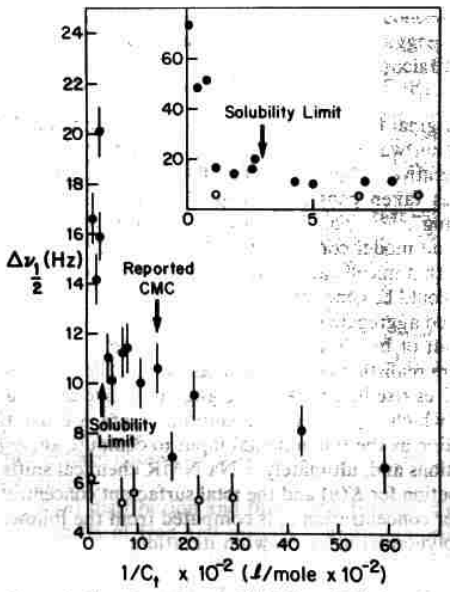

Figure 3. Concentration dependence of ^{23}Na line width $\Delta\nu_{1/2}$ for aqueous SHBS solutions (●) and for aqueous NaCl solutions (○) at 47 °C.

symmetric and Lorentzian. At concentrations above the solubility limit, the ^{23}Na NMR line shapes are asymmetric with a shoulder downfield of the main peak. Figure 2 shows clearly the presence of two overlapping resonance peaks in a 0.354 wt % SHBS in water solution (c_t = 8.77 × 10^{-3} M), a concentration at which about 60% of the surfactant is in the lamellar phase and 40% in the isotropic though aggregated surfactant solution. The overall signal can be decomposed into a superposition of two Lorentzian lines whose line widths agree well with those of the saturated isotropic and the lamellar phases, ca. 16 and 70 Hz, respectively. In this reconstruction, we have weighted the two Lorentzians by the respective weight fractions of saturated isotropic and lamellar phase, 0.4 and 0.6. Here we neglect the distribution of sodium counterions relative to surfactant in isotropic and lamellar phases and assume they distribute in proportion to surfactant concentrations. A plot of line width vs. inverse concentration (Figure 3) delineates clearly the phase transition. Below the solubility limit, the line widths change continuously, ultimately approaching the value for dilute electrolyte at the lowest concentration measured. At concentrations above the solubility limit but for which a significant fraction of the SHBS is still in isotropic solution,

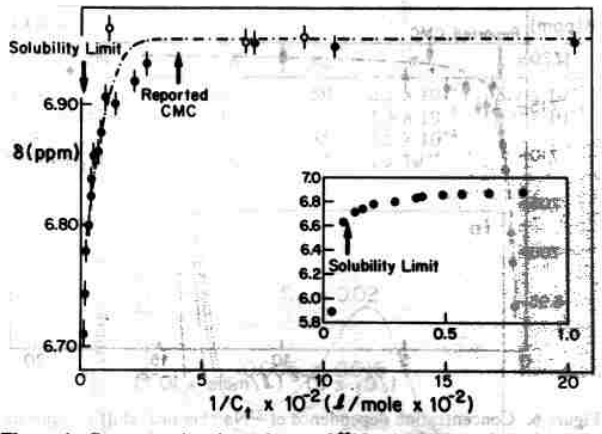

Figure 4. Concentration dependence of ^{23}Na chemical shift in aqueous Aerosol OT solutions (●) and aqueous NaCl solutions (○) at 47 °C, with turbidity-determined solubility limit and reported[1,2] cmc (at 20 °C) indicated. The dashed line was calculated by using $K(n) = 700 \exp(-1.5 \times 10^{-3}(n-25)^2)$.

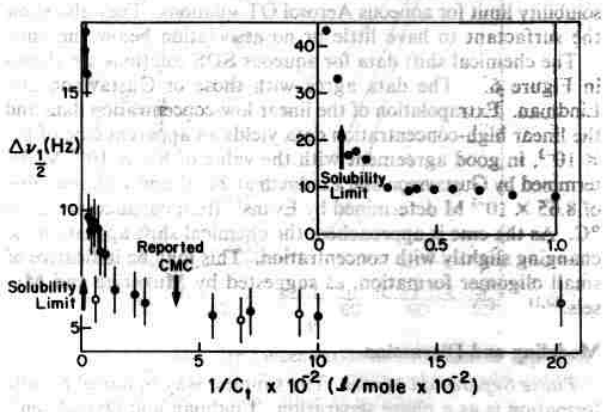

Figure 5. Concentration dependence of ^{23}Na line widths in aqueous Aerosol OT solutions at 47 °C. The solubility limit, the line half-width of aqueous NaCl solutions at 47 °C, and the reported cmc (at 20 °C) are indicated.

both the chemical shift, defined as the position of observed maximum signal intensity, and the line widths are functions of the surfactant inventory, as well as the line widths and relative positions of the two Lorentzians. They do not vary with concentration in a simple manner.

Both chemical shift and line-width data indicate the presence of a solubility limit at ca. 3.3 × 10^{-3} M. Below this concentration, the counterion's average environment changes smoothly and continuously, indicating non- or anticooperative small aggregate formation, not micellization.

A similar set of ^{23}Na NMR chemical shift (Figure 4) and line-width (Figure 5) measurements were made on Aerosol OT–water samples. Both sets of data have three distinct features: (1) below the reported cmc (400 M^{-1}) the chemical shift and line width are independent of concentration and identical with those of dilute NaCl solutions within experimental uncertainty; (2) between the cmc and the visually determined solubility limit (10 M^{-1}) the chemical shift and line width change monotonically; and (3) above the solubility limit the chemical shift and line width change rapidly as concentration increases. The ^{23}Na line shapes of Aerosol OT solutions above the solubility limit are similar to those of SHBS above its solubility limit. The concentration independence of chemical shift and line width below 2.5 × 10^{-3} M suggests Aerosol OT is unassociated and behaves as a dilute electrolyte. The smooth and monotonic decrease in chemical shift and increase in line width above this concentration are consistent with micelle formation as deduced from data by surface tension[1,2] and conductance[3] measurements at room temperature. Above the observed solubility limit, both chemical shift and line width change rapidly. The ^{23}Na

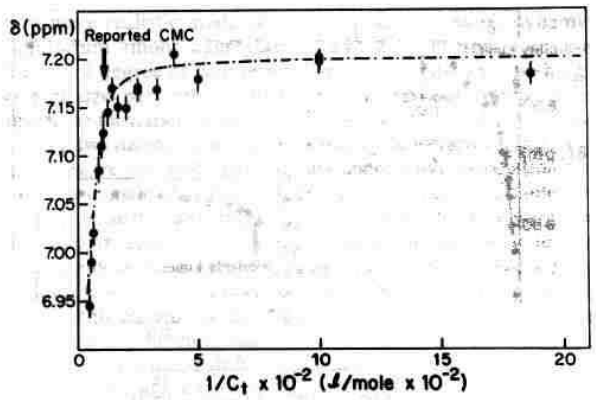

Figure 6. Concentration dependence of ^{23}Na chemical shift in aqueous SDS solutions at 25 °C. Also shown is the reported[19] cmc determined by conductance at 40 °C. The dashed line was calculated by using $K(n) = 700 \exp(-2.5 \times 10^{-4}(n - 50)^2)$.

spectroscopic data thus delineate well both the cmc and the solubility limit for aqueous Aerosol OT solutions. They also show the surfactant to have little or no association below the cmc.

The chemical shift data for aqueous SDS solutions are shown in Figure 6. The data agree with those of Gustavsson and Lindman. Extrapolation of the linear low-concentration data and the linear high-concentration data yields an apparent cmc of 8.7×10^{-3}, in good agreement with the value of 8.6×10^{-3} M determined by Gustavsson and Lindman at 28 °C and with the value of 8.65×10^{-3} M determined by Evans[19] from conductivity at 40 °C. As the cmc is approached, the chemical shift appears to be changing slightly with concentration. This may be indicative of small oligomer formation, as suggested by Mukerjee and Mysels.[20,21]

Modeling and Discussion

Phase Separation Model. The simplest way to model micelle formation is as a phase separation. Lindman and Danielsson[18] and later Gustavsson and Lindman[15,16] have shown that treating micellization in this way leads to eq 1 for the observed chemical shift above the cmc. The phase separation model assumes that below the cmc only monomers exist and the observed chemical shift is concentration independent while above the cmc all additional surfactant is incorporated in aggregates of infinite size. The model further assumes that the fractional degree of counterion binding, β, is independent of concentration. This leads to the linear dependence of the observed chemical shift on inverse surfactant concentration. Clearly, this is an oversimplification and only approximates the chemical shift data at concentrations far below and far above the cmc. In these respects, the model is useful for obtaining δ_f and δ_b, the limiting values of monomer and micellar ^{23}Na chemical shift. An improvement on this model in the vicinity of the cmc can be made by assuming aggregates of finite size.

Bury–Hartley Model. The Bury–Hartley model[22,23] assumes dynamic equilibrium between two species—monomer and monodisperse micelle:

$$nq_1 = q_n \qquad K = c_n/c_1^n \tag{2}$$

Here, n is the aggregation number, q_1 and q_n are monomer and micelle, c_1 and c_n are their concentrations, and K is the equilibrium constant which describes the equilibrium populations. By taking δ_f to be the chemical shift of free counterion and δ_b the chemical shift of micelle-bound counterion and by assuming that the fractional degree of counterion binding, β, is concentration independent, we can plot log $(c_t\delta)$ vs. log $(c_t(\delta_b^* - \delta))$ and obtain the aggregation number n as slope.[24-27] From Figure 6, $\delta_f = 7.20$ is the chemical shift of free counterions at 25 °C and $\delta_b^* = 6.76$ is the chemical shift of bound counterions weighted by the fractional degree of counterion binding (δ_b^* is obtained by extrapolating the high concentration chemical shift data to $1/c_t = 0$). A linear least-squares fit to the chemical shift data for SDS yields an aggregation number of 5 at the cmc. *However, SDS in water is known[28] to have a micellar aggregation number of 60–70 and not 5.* Although it is an improvement on the phase separation model, the Bury–Hartley model is too simple to accurately predict the variation of counterion chemical shift data near the cmc. Three factors could contribute to the discrepancy: polydispersity in micelle aggregation number, premicellar aggregation, and a size- as well as concentration-dependent β. We consequently considered an association model which accommodates these factors.

Mass Action Model. A multiple equilibrium mass action model has been used by many authors to predict surfactant association in water.[29-33] Aggregation is treated as a stepwise addition process governed by a set of equilibrium constants:

$$\begin{aligned} q_1 + q_1 &= q_2 \qquad K_2 = c_2/c_1^2 \\ q_1 + q_2 &= q_3 \qquad K_3 = c_3/K_2c_1^3 \\ &\cdots \qquad \cdots \\ q_1 + q_{n-1} &= q_n \qquad K_n = c_n/K_{n-1} \cdots K_2c_1^n \end{aligned} \tag{3}$$

In the original treatment of Meyer and van der Wyk,[29] the $K(n)$ distribution was constant; i.e., the association was completely noncooperative, $dK(n)/dn = 0$ for all n. In a subsequent treatment, $K(n)$ was taken constant except for $K(2)$, i.e. "dimerization controlling".[31,32] This is a specific example of a more general association model considered by Bidner et al.[33] Their analysis revealed that micelle inventories and moments of the aggregation number could be generated with a step-function $K(n)$ distribution. Calculated aggregate size distributions were, however, unrealistic as a result of building all cooperativity into a step change.

A more realistic mass action model of micelle formation is one which gives rise to a peak in the aggregate size distribution, i.e. one for which $K(n)$ has a maximum. Here, we use the $K(n)$ distribution as the fundamental input to compute aggregate size distributions and, ultimately, ^{23}Na NMR chemical shifts. Given a distribution for $K(n)$ and the total surfactant concentration, the monomer concentration c_1 is computed from the following Nth-order polynomial using Newton iteration:

$$c_t = c_1 + \sum_{i=2}^{N} i \prod_{j=2}^{i} K_j c_1^i \tag{4}$$

Here, c_t is the total surfactant concentration and the sum is truncated at a sufficiently large aggregate size N such that the inventory of surfactant in aggregates larger than N is negligible. Once the monomer concentration is calculated, all aggregate size concentrations are readily computed from eq 3. This monomer concentration is then used as an initial approximation in iterating for c_t at the next larger surfactant concentration. Further details on our use of the method can be found in Kilpatrick et al.[34]

(19) H. C. Evans, *J. Chem. Soc.*, 577 (1956).
(20) P. Mukerjee and K. J. Mysels, *J. Phys. Chem.*, **61**, 1400 (1957).
(21) P. Mukerjee, *J. Phys. Chem.*, **69**, 2821 (1965).
(22) E. R. Jones and C. R. Bury, *Philos. Mag.*, **4**, 841 (1927).
(23) R. C. Murray and G. S. Hartley, *Trans. Faraday Soc.*, **31**, 183 (1935).
(24) B.-O. Persson, T. Drakenberg, and B. Lindman, *J. Phys. Chem.*, **80**, 2124 (1976).
(25) B.-O. Persson, T. Drakenberg, and B. Lindman, *J. Phys. Chem.*, **83**, 3011 (1979).
(26) N. Muller and R. H. Birkhahn, *J. Phys. Chem.*, **71**, 957 (1967).
(27) N. Muller and T. W. Johnson, *J. Phys. Chem.*, **73**, 2042 (1969).
(28) K. J. Mysels and L. H. Princen, *J. Phys. Chem.*, **63**, 1696 (1959).
(29) K. H. Meyer and A. Van der Wyk, *Helv. Chim. Acta*, **20**, 1321 (1937).
(30) J. M. Corkill, J. F. Goodman, T. Walker, and J. Wyer, *Proc. R. Soc. London, Ser. A*, **312**, 243 (1969).
(31) F. J. C. Rossotti and H. Rossotti, *J. Phys. Chem.*, **65**, 926 (1961).
(32) A. K. Ghosh and P. Mukerjee, *J. Am. Chem. Soc.*, **92**, 6408 (1972).
(33) M. S. Bidner, R. G. Larson, and L. E. Scriven, *Lat. Am. J. Chem. Eng. Appl. Chem.*, **6**, 1 (1976).

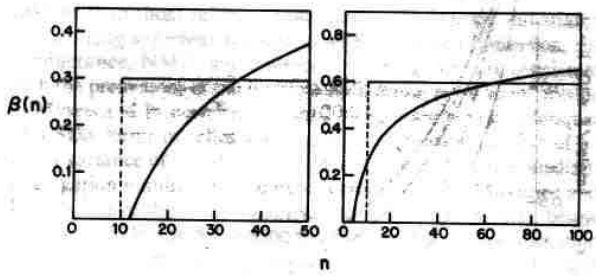

Figure 7. Assumed functional dependence of fractional degree of counterion binding, β, on aggregate size n: (a) constant surface charge density with $\beta(35) = 0.3$ or a step function, for SHBS and Aerosol OT, and (b) constant surface charge density with $\beta(65) = 0.6$ or a step function, for SDS.

As one of the simplest forms of a $K(n)$ distribution with a global maximum, we use a Gaussian distribution:

$$K(n) = K_0 \exp(-a(n - n_0)^2) \quad (5)$$

The value of K_0 does not affect the cooperativity of association but only shifts the concentration range over which aggregation takes place. The value of n_0 determines the aggregate size of greatest concentration at large overall surfactant concentrations while the value of a controls the variance of the aggregate size distribution and the degree of cooperativity of association. We have also considered $K(n)$ distributions which are a superposition of a half-Gaussian to describe anticooperative small aggregate formation and a Gaussian to model large aggregate formation.[34]

Once a $K(n)$ distribution has been selected, the dependence of fractional counterion binding, β, on aggregate size must be modeled. We have considered two cases: (1) spherical aggregates with uniformly distributed counterions over the aggregate surface, which give rise to constant surface charge density, and (2) a step-function change in β with aggregate size. With $K(n)$ distributions giving rise to large aggregate sizes and with few aggregates of intermediate size, chemical shifts calculated by using the two β dependences agree closely, reflecting the slowly varying β for case 1 at large n. With non- and anticooperative $K(n)$ distributions giving rise to a broadly distributed and skewed small aggregate population, the calculated chemical shifts are a sensitive function of the form chosen for β. The two cases considered are shown in Figure 7.

With the $K(n)$ distribution and functional form of β chosen, the chemical shifts of free and micelle-bound counterions are determined by linear extrapolation of the high- and low-concentration chemical shift data. Chemical shifts are then computed by calculating the fraction of free and of bound counterions and assuming the observed chemical shift is a number-weighted average of the two populations:

$$\delta = \frac{c_1 + \sum_{i=2}^{N} i(1 - \beta(i))c_i}{c_t}\delta_f + \frac{\sum_{i=2}^{N} i\beta(i)c_i}{c_t}\delta_b \quad (6)$$

Comparison of Model and Experimental Data. The ^{23}Na NMR chemical shift of free counterion, δ_f, is obtained by extrapolating the experimental data to infinite dilution. With SDS at 25 °C, $\delta_f = 7.20$ ppm while for SHBS and Aerosol OT at 47 °C, $\delta_f = 6.955$ ppm. These are also, of course, the chemical shifts of dilute NaCl solutions at each temperature. The ^{23}Na NMR chemical shifts of the aggregate-bound counterion are obtained by a linear extrapolation of the experimental data on an inverse concentration scale over concentrations greater than the reported cmc and less than the solubility boundary. This yields the product of δ_b and β at large concentrations. With single-tail anionic surfactants, β has been found to vary from 0.5 to 0.8. In our model calculations for SDS, we have used a value for β of 0.6 for an aggregate size of 65, i.e. $\beta(65) = 0.6$. With double-tail surfactants, β is typically smaller,[35] as are the aggregate sizes.[35,36] Accordingly, we have chosen a value for β of 0.3 for SHBS and Aerosol OT at an aggregate size of 35. These choices are not unique, and the model chemical shift data can be adequately matched to the experimental data by using other mean aggregate sizes and β's.

Once a limiting value of β is chosen, δ_b can be calculated. For SDS, it is 6.46 ppm or $\delta_f - \delta_b = 0.74$ ppm. For Aerosol OT, $\delta_b = 6.175$ ppm and $\delta_f - \delta_b = 0.78$ ppm. The high-concentration chemical shift data for SHBS, below the solubility limit, are not linear and when extrapolated to $1/c_t = 0$, yield a low value of $\delta_f - \delta_b$. We have therefore used the same values of δ_b in modeling both Aerosol OT and SHBS chemical shift data.

The maximum in the equilibrium large aggregate concentration as a function of aggregate size is greater than the maximum in the Gaussian $K(n)$ distribution. Accordingly, a n_0 was taken to be 50 for modeling the SDS data and 25 for modeling SHBS and Aerosol OT. Once n_0 was chosen, the value of a was adjusted until the curvature at the cmc for the calculated chemical shift approximated that of the experimental data. Finally, K_0 was adjusted until the calculated data matched the experimental data. With a few exceptions, the calculated values matched the experimental data within the uncertainty of the measurements in all three surfactant systems. The calculated chemical shifts are represented by dashed lines in Figure 1, 4, and 6. The values of K_0, n_0, and a in eq 5 used to fit the data for the three cases, along with apparent cmcs, are given in Table I.

The $K(n)$ distributions of the stepwise association processes which best match the SDS and Aerosol OT chemical shift data

TABLE I

system	K	n_0	a	cmc, M
SDS–H_2O	700	50	2.5×10^{-4}	8.7×10^{-3}
Aerosol OT–H_2O	700	25	1.5×10^{-3}	8.0×10^{-3}
SHBS–H_2O	3.0×10^4	25	3.0×10^{-4}	
SHBS–H_2O	5.0×10^4	2	1×10^{-5}	

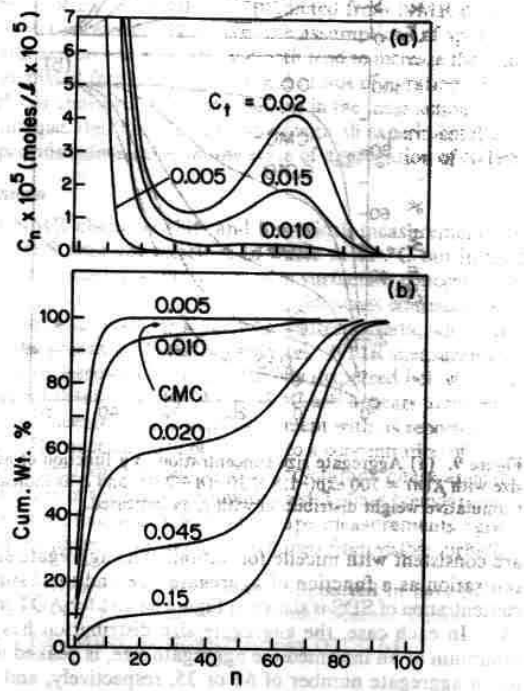

Figure 8. (a) Aggregate size concentration as a function of aggregate size with $K(n) = 700 \exp(-2.5 \times 10^{-4}(n - 50)^2)$ and c_t as indicated. (b) Cumulative weight distribution with c_t as indicated.

(34) P. K. Kilpatrick, H. T. Davis, W. G. Miller and L. E. Scriven, to be submitted for publication.

(35) R. Zana, *J. Colloid Interface Sci.*, 78, 330 (1980).
(36) D. Schmidt, Ch. Gahwiller, and C. Von Planta, *J. Colloid Interface Sci.*, 83, 191 (1981).

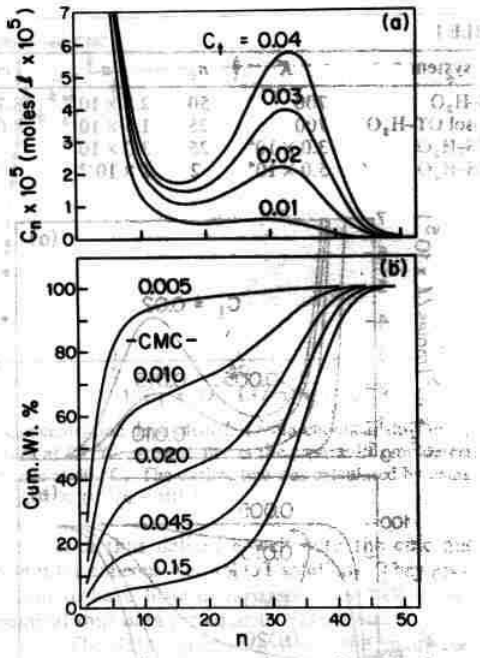

Figure 9. (a) Aggregate size concentration as a function of aggregate size with $K(n) = 700 \exp(-1.5 \times 10^{-3}(n-25)^2)$ and c_t as indicated. (b) Cumulative weight distribution with c_t as indicated.

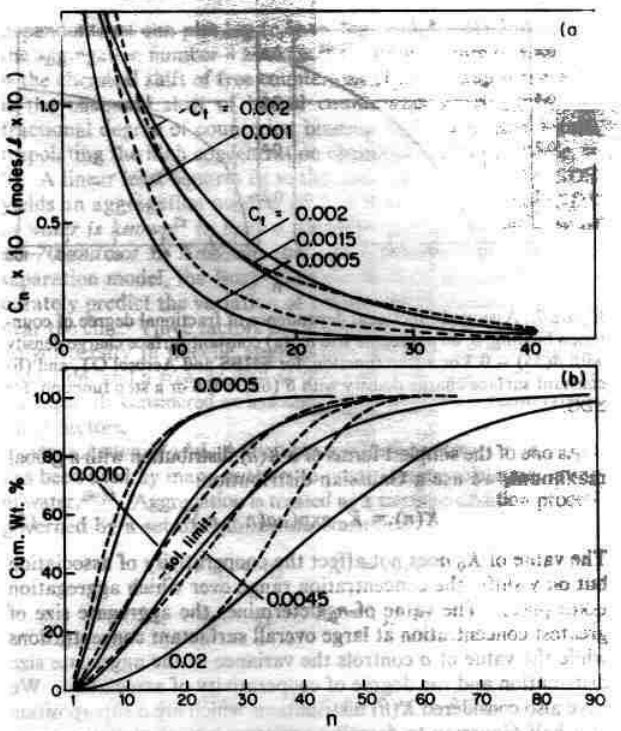

Figure 10. (a) Aggregate size concentration as a function of aggregate size with $K(n) = 5 \times 10^4 \exp(-1 \times 10^{-5}(n-2)^2)$, solid line, and with $K(n) = 3 \times 10^4 \exp(-3 \times 10^{-4}(n-25)^2)$, dashed line, at different values of c_t. (b) Cumulative weight distribution with c_t as indicated.

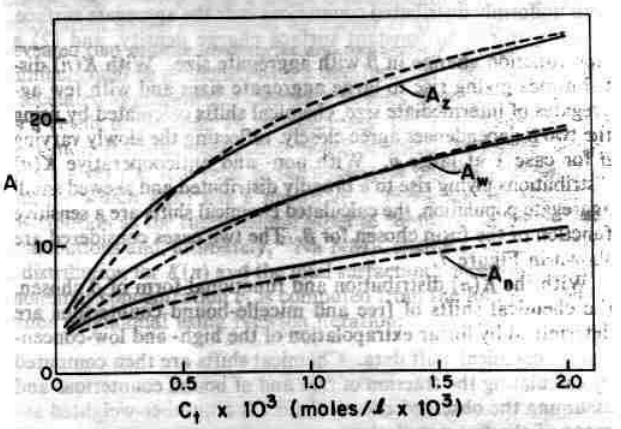

Figure 11. Moments of the aggregation number vs. total surfactant concentration for the two $K(n)$ distributions of Figure 10.

are consistent with micelle formation. The aggregate size concentration as a function of aggregate size and total surfactant concentration of SDS is shown in Figure 8a and for AOT in Figure 9a. In each case, the aggregate size distribution has a local minimum at an intermediate aggregate size, is peaked near the mean aggregate number of 65 or 35, respectively, and rapidly decreases at larger aggregate sizes. At the total surfactant concentrations shown in Figures 8a and 9a, the concentration of small aggregates, $n < 10$, is larger than the proper micelle concentration. This is expected near the cmc, but as the total concentration increases, the micelle concentration ultimately overtakes the small oligomer concentration. The corresponding cumulative surfactant inventories, Figures 8b and 9b, further show this behavior.

With use of the aforementioned δ_b value and the $\beta(n)$ distribution, the SHBS data could only be matched by taking a to be quite small, 3.0×10^{-4}, i.e. with a large variance in the $K(n)$ distribution. The resulting aggregate distribution shows no maximum in large aggregate size with concentrations up to the solubility limit; i.e., micelles do not form. Instead, the aggregate concentrations decrease monotonically with increasing aggregate size (Figure 10). The SHBS chemical shift data were fit equally well by taking $n_0 = 2$, $a = 1 \times 10^{-5}$, and $K_0 = 5.0 \times 10^{-4}$. This model is anticooperative except for dimer formation. Again the aggregate size distribution showed no maximum up to the solubility limit (Figure 10). This result indicates that two $K(n)$ distributions, one which is weakly anticooperative and one which is weakly cooperative, can model the chemical shift data equally well. Nonetheless, the resulting aggregate size distribution over the concentration range of interest is similar for the two cases. It is these aggregate size profiles which reflect the degree of cooperativity of the association in the three systems examined. In contrast to the choice of $\beta(n)$ in fitting the model to SDS and AOT data, the form of $\beta(n)$ for the SHBS data had a significant effect on the best-fit parameters. Nevertheless, the resulting aggregate size distribution did not show a maximum large aggregate size at concentrations below the solubility limit. Thus, the SHBS data can be fit by using a variety of $K(n)$ and $\beta(n)$ distributions, but the resulting aggregate size distribution is virtually the same.

The $K(n)$ distributions used to model both the SDS and the Aerosol OT data predict a peak in the aggregate size distribution, with a most probable size of 65 and a variance of 14 for SDS, and 33 and 8, respectively, for AOT, at concentrations well above the cmc. These distributions are consistent with closed aggregates of large size, i.e. micelles. The $K(n)$ distributions used to model the SHBS data predict a monotonically decreasing aggregate size and hence no cooperativity or closure. The $K(n)$ distributions indicate weak, non-, or anticooperative association in the SHBS–water system, not micelle formation. In the light of the fit of the SHBS data to the $K(n)$ distribution with $n_0 = 25$, we cannot conclude that SHBS would not form micelles at sufficiently high concentrations if the solubility limit did not intercede; the calculated distributions, when extended considerably beyond the solubility limit, show a maximum in large aggregate size. This suggests that SHBS may indeed micellize at higher temperatures above its Krafft boundary, if those temperatures could be reached before the surfactant degraded. Although the SHBS aggregate distribution determined in fitting the NMR data does not show micellar behavior up to the solubility limit, the z-average aggregate size is in excess of 20 (Figure 11) in the concentration range investigated by neutron scattering.[13] Although these values are

smaller than those inferred from neutron scattering, calculated by assuming spherical aggregates with no water penetration, the conductance, NMR, and neutron scattering data are consistent with the predictions of the multiple equilibrium mass action model.

Mysels and Princen[28] established by light scattering techniques that SDS forms micelles with a mean aggregation number of 62 and a variance of about 10. Fitting our NMR data to a medium aggregation number of 65 yields a variance of 14. Mukerjee and Mysels[20] have shown by conductance measurements that, below the cmc of SDS (ca. 8.5×10^{-3} M), there is measurable formation of small oligomers. They inferred this from a slope of equivalent conductivity vs. the square root of surfactant concentration greater than that predicted by Onsager limiting law behavior. The best mass action model fit to the SDS data also shows a small fraction of surfactant inventory in oligomers below the cmc (Figure 8a).

Williams et al.[1] and Rudenko et al.[2] argued from the break in slope of surface tension vs. the logarithm of surfactant concentration that Aerosol OT micellizes. Although the break is abrupt, which indicates cooperativity of association, the surface tension continues to decrease beyond the cmc, which indicates small aggregation numbers. Both cooperativity of association and small aggregation numbers are consistent with our model fit, although the cumulative surfactant inventory (Figure 9b) indicates the cooperativity of association is less than that for SDS. The conductance data of Fontell[3] is also consistent with small aggregation numbers, because there is an abrupt but small change in slope of equivalent conductivity with the square root of surfactant concentration.

All experimental data on SHBS are consistant with non- or anticooperative surfactant association, not micelle formation. Conductance data[10,12] show a continuous variation of equivalent conductivity greater than that predicted by the Onsager limiting law. Moreover, there is no evidence of a break in slope of equivalent conductivity. This is in stark contrast to the SDS data and measurably different from the Aerosol OT data[3] which show breaks consistent with micelle formation and slopes in agreement with Onsager limiting law below the breaks. The neutron scattering data of Magid et al.[13] give an apparent hydrodynamic radius of ca. 23 Å. By assuming spherical surfactant aggregates with no water penetration, we calculate an apparent z-average aggregation number (A_z) of about 65 from their data. This is larger than the A_z of 20–30 (Figure 11) predicted from NMR data by the mass action model. However, the assumptions of spherical aggregates and no water penetration both tend to increase the value of A_z calculated from the experimental radius of gyration. Thus, although our choices of $K(n)$ distributions in the mass action model are not unique, they are fully consistent with all experimental data which provide information on the state of aggregation of SHBS.

Conclusions

^{23}Na NMR chemical shift and line-width measurements indicate SHBS does not micellize in water at 47 °C but instead continuously associates with increase in surfactant concentration to form small aggregates. The NMR evidence is consistent with conductance and small-angle neutron scattering data, which also indicate the presence of small aggregates. NMR measurements also indicate Aerosol OT is molecularly dispersed below a concentration of about 2.5×10^{-3} M at 47 °C and appears to micellize above that concentration, in good agreement with its reported cmc at 20 °C. The micellar state persists up to a concentration of about 0.10 M, whereupon a lamellar liquid-crystalline phase appears. Determination of the isotropic–liquid–crystal phase boundary with chemical shift, line-width, and line-shape measurements agrees well with the phase boundary as determined from visible turbidity.

Acknowledgment. This work was supported in part by the Department of Energy and the National Science Foundation.

Registry No. SHBS, 67267-95-2; Aerosol OT, 577-11-7.